IUTAM Symposium Analytical Methods in Nonlinear Dynamics

Dynamics of a Delay Limit Cycle Oscillator with Self-Feedback

Lauren Lazarus[a], Matthew Davidow[b], Richard Rand[a,c]

[a]Dept. Mechanical and Aerospace Engineering, Cornell University
[b]Center for Applied Mathematics, Cornell University
[c]Dept. of Mathematics, Cornell University

Abstract

This paper concerns the dynamics of the following nonlinear differential-delay equation:

$$\dot{x} = -x(t - T) - x^3 + \alpha x$$

in which T is the delay and is a coefficient of self-feedback. Using numerical integration, continuation programs and bifurcation theory, we show that this system exhibits a wide range of dynamical phenomena, including Hopf and pitchfork bifurcations, limit cycle folds and relaxation oscillations. It is shown that this equation governs the in-phase and out-of-phase motions of a system of two coupled nonlinear differential-delay equations.

© 2016 The Authors. Published by Elsevier B.V. This is an open access article under the CC BY-NC-ND license
(http://creativecommons.org/licenses/by-nc-nd/4.0/).
Peer-review under responsibility of organizing committee of IUTAM Symposium Analytical Methods in Nonlinear Dynamics

Keywords: delay differential equation ; self-feedback; limit cycle; relaxation-oscillation; perturbation

1. Introduction

Coupled oscillators have long been an area of interest in Nonlinear Dynamics. An early effort involved two coupled van der Pol oscillators [1,2,3,4,5]. Related work involved coupling two van der Pol oscillators with delayed terms [6].

Besides van der Pol oscillators, other models of coupled limit cycle oscillators have been studied. An important class consists of "phase-only oscillators". These have been studied using algebraic coupling [7,8,9,10,11] as well as delayed coupling [12].

Recent interest in dynamical systems with delay has produced a new type of oscillator which has the form of a differential-delay equation (DDE):

$$\dot{x} = -x(t - T) - x^3 \tag{1}$$

E-mail address: rand@math.cornell.edu

As we shall see, this system exhibits a Hopf bifurcation at $T = \pi/2$ in which a limit cycle is born[13,14]. We shall refer to Eq. (1) as a "delay limit cycle oscillator".

The present work is motivated by a study of the dynamics of a system of two coupled delay limit cycle oscillators, each of the form of Eq. (1):

$$\dot{x} = -x(t - T) - x^3 + \alpha y \tag{2}$$
$$\dot{y} = -y(t - T) - y^3 + \alpha x \tag{3}$$

where $x, y \in \mathbb{R}$.

In particular it will be the focus of this study to examine the dynamics of the in-phase mode, $x = y$. Flow on this invariant manifold satisfies the DDE:

$$\dot{x} = -x(t - T) - x^3 + \alpha x \tag{4}$$

Eq. (4), which may be described as a delay limit cycle oscillator with self-feedback, is the subject of this paper[18].

2. Equilibria and their Stability

Equilibria in Eq. (4) are given by the equation

$$0 = -x - x^3 + \alpha x \tag{5}$$

For $\alpha < 1$, only $x = 0$ is a solution. For $\alpha \geq 1$, an additional pair of solutions $x = \pm\sqrt{\alpha - 1}$ exist such that there are 3 constant solutions. These solutions emerge from the $x = 0$ solution in a pitchfork bifurcation at $\alpha = 1$. See Fig. 1(a).

In order to determine the stability of the equilibrium at $x = 0$, we investigate the linearized DDE:

$$\dot{x} = -x(t - T) + \alpha x \tag{6}$$

Setting $x = Ae^{\lambda t}$, we obtain the characteristic equation:

$$\lambda = -e^{-\lambda T} + \alpha \tag{7}$$

In the non-delay ($T = 0$) case, we are left with $\lambda = \alpha - 1$; therefore $x = 0$ is stable for $\alpha < 1$ and becomes unstable for $\alpha > 1$ where the other equilibria (the arms of the pitchfork) exist. See Fig. 1(a).

For non-zero delay ($T > 0$), we anticipate the existence of a Hopf bifurcation and the creation of a limit cycle, based on the known behavior for $\alpha = 0$. We look for pure imaginary eigenvalues by substituting $\lambda = i\omega$ into the characteristic equation (7) and separating the real and imaginary terms into separate equations:

$$\omega = \sin(\omega T) \tag{8}$$
$$0 = -\cos(\omega T) + \alpha \tag{9}$$

By manipulating these we obtain:

$$\sin^2(\omega T) + \cos^2(\omega T) = \omega^2 + \alpha^2 = 1 \tag{10}$$

$$T_H = \frac{\arccos \alpha}{\omega} = \frac{\arccos \alpha}{\sqrt{1 - \alpha^2}} \tag{11}$$

So for a given α, there exists a delay T_H where a Hopf bifurcation occurs at $x = 0$. In this case, the Hopf bifurcation only exists for $-1 < \alpha < 1$, in order for ω to be real and T_H to be finite. Note that for $\alpha = 0$ (which corresponds to the uncoupled oscillator of Eq. (1)), the Hopf occurs at $T_H = \pi/2$. Fig. 1(b) shows the stability of the $x = 0$ equilibrium point in α-T space.
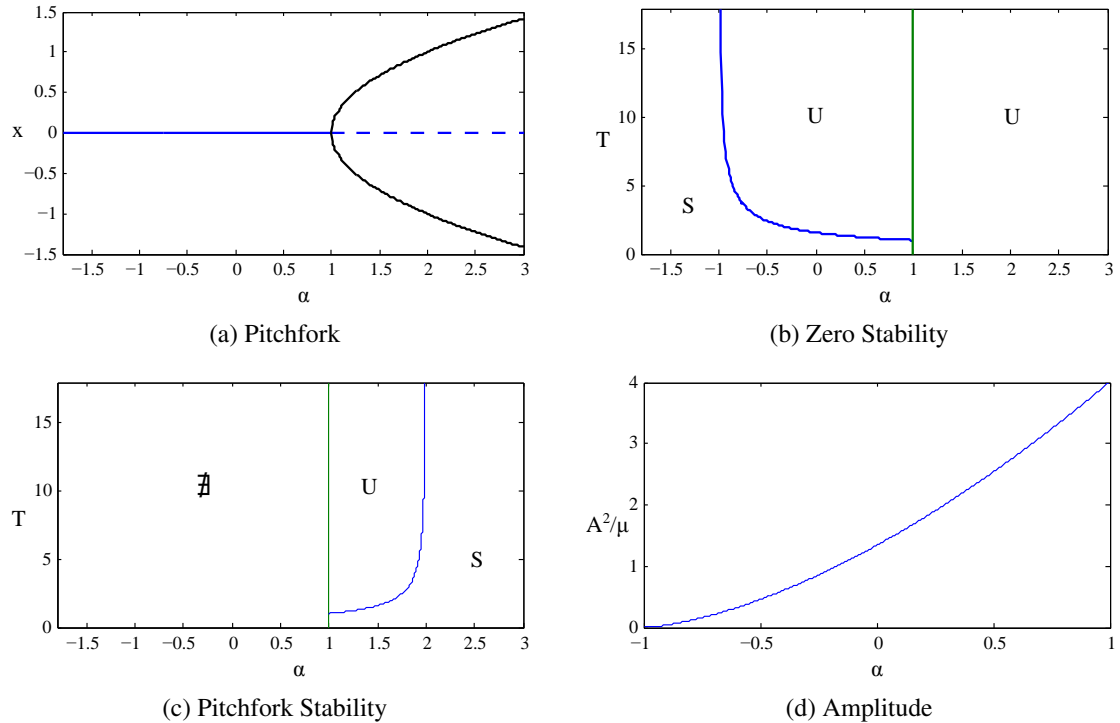
(a) Pitchfork

(b) Zero Stability

(c) Pitchfork Stability

(d) Amplitude

Fig. 1. (a) Locations of equilibria as a function of α, independent of T; (b) Stability diagram for the equilibrium at $x = 0$. Regions respectively represent stable (S) and unstable (U). The curved line is given by the Hopf Eq. (11). The instability for $\alpha > 1$ is due to a pitchfork bifurcation; (c) Stability diagram for the equilibria at $x = \pm\sqrt{\alpha - 1}$. Regions respectively represent nonexistence ($\nexists$), unstable (U) and stable (S). The curved line is given by the Hopf Eq. (15); (d) The coefficient of μ in Eq. (17) is plotted for $-1 < \alpha < 1$. Its non-negative value shows that the limit cycle is stable, see text.

Next we consider the stability of the equilibria located along the arms of the pitchfork at

$$x = \pm\sqrt{\alpha - 1} \tag{12}$$

We begin by setting $x = \pm\sqrt{\alpha - 1} + z$, where z represents a small deviation from the equilibrium. This gives the following nonlinear DDE:

$$\dot{z} = -z(t - T) + (3 - 2\alpha)z \mp 3\sqrt{\alpha - 1}z^2 - z^3 \tag{13}$$

Stability is determined by linearizing this equation about $z = 0$:

$$\dot{z} = -z(t - T) + (3 - 2\alpha)z \tag{14}$$

Note that this is the same as Eq. (6) with α replaced by $3 - 2\alpha$. Thus we use Eq. (11) to find the critical delay for Hopf bifurcation as:

$$T_H = \frac{\arccos(3 - 2\alpha)}{\sqrt{1 - (3 - 2\alpha)^2}} \tag{15}$$

Fig. 1(c) shows the existence and stability of the equilibria located at $x = \pm\sqrt{\alpha - 1}$.

3. Limit Cycles

As demonstrated in the foregoing analysis, Eq. (4) exhibits multiple curves of Hopf bifurcations, each generically yielding a limit cycle. We are concerned about the following questions regarding these limit cycles:

a) are they stable, i.e. are the Hopf bifurcations supercritical?

b) what happens to the limit cycles away from the Hopf bifurcations?

The question of the stability of the limit cycles may be answered by applying the multiple scales perturbation method to the nonlinear DDEs (4) and (13). In fact this has already been accomplished for a general DDE of the form [15]:

$$\frac{du}{dt} = \gamma u + \beta u_d + a_1 u^2 + a_2 u u_d + a_3 u_d^2 + b_1 u^3 + b_2 u^2 u_d + b_3 u u_d^2 + b_4 u_d^3 \tag{16}$$

where $u = u(t)$ and $u_d = u(t - T)$. When the results of reference [15] are applied to Eq. (4), we find that the amplitude A of the limit cycle is given by the expression:

$$A^2 = \frac{-4(\alpha^2 - 1)^2}{3(\alpha \sqrt{1 - \alpha^2} \arccos \alpha + \alpha^2 - 1)} \mu \tag{17}$$

where μ is the detuning off of the critical delay,

$$T = T_H + \mu, \tag{18}$$

and where the approximate form of the limit cycle is $x = A \cos \omega t$. Here T_H and ω are given by Eqs. (10) and (11). A plot of the coefficient of μ in Eq. (17) is given in Fig. 1(d) for $-1 < \alpha < 1$. Note that this coefficient is non-negative over this parameter range (cf. Fig. 1(b)), which means that the limit cycle occurs for positive μ, i.e. for $T > T_H$, i.e. when the equilibrium at $x = 0$ is unstable. Since the Hopf occurs in a 2-dimensional center manifold, this shows that the Hopf is supercritical and the limit cycle is stable.

A similar analysis may be performed for limit cycles born from equilibria located on the arms of the pitchfork bifurcation. In this case we use Eq. (13) and find that the limit cycle is unstable, and that the Hopf is subcritical.

These results have been confirmed by comparison with numerical integration of Eq. (4) using the MATLAB function DDE23 and the continuation software DDE-BIFTOOL [16,17]. Fig. 2(a) shows a limit cycle obtained by using DDE23 for delay $T=4$ and $\alpha=-0.75$. For these parameters, Eq. (11) gives $T_H=3.6570$ and Eq. (17) gives a limit cycle amplitude of $A=0.2312$. Also, Eq. (10) gives $\omega=0.6614$, which gives a period of $2\pi/\omega=9.4993$. Note that these computed values agree with the values obtained by numerical simulation in Fig. 2(a).

The DDE-BIFTOOL software shows that the limit cycles born in a Hopf from the equilibrium at $x = 0$, die in a limit cycle fold. Fig. 2(b) displays two BIFTOOL plots of limit cycle amplitude ($\times$ 2) versus α for $T = 1.1$ and $T = 3.5$. The collection of all such curves is a surface in α-T-Amplitude space and is displayed in Fig. 2(c). Note that although the locus of limit cycle fold points is not found analytically here, an approximation is obtained from the DDEBIFTOOL curves which is shown in Fig. 2(c). When projected down onto the α-T plane, it represents the boundary beyond which there are no stable limit cycles.

As noted above, the Hopf bifurcations acting on the equilibria located on the arms of the pitchfork are subcritical, i.e. the resulting limit cycle is unstable. This is illustrated in Fig. 2(d) which is a BIFTOOL computation showing the Hopf bifurcation at $\alpha = 1.5$ for varying delay T. Eq. (15) gives the critical value $T_H = \pi/2$.

4. Large Delay

Numerical simulation of Eq. (4) shows that for large values of delay, the limit cycles become relaxation oscillations, that is, they take the form of an approximate square wave, see Fig. 3(a). The following features have been observed in numerical simulations (cf. Fig. 3(a)):

- The period of the square wave is approximately equal to the delay T.
- The amplitude of the square wave is approximately equal to $\sqrt{1 + \alpha}$.
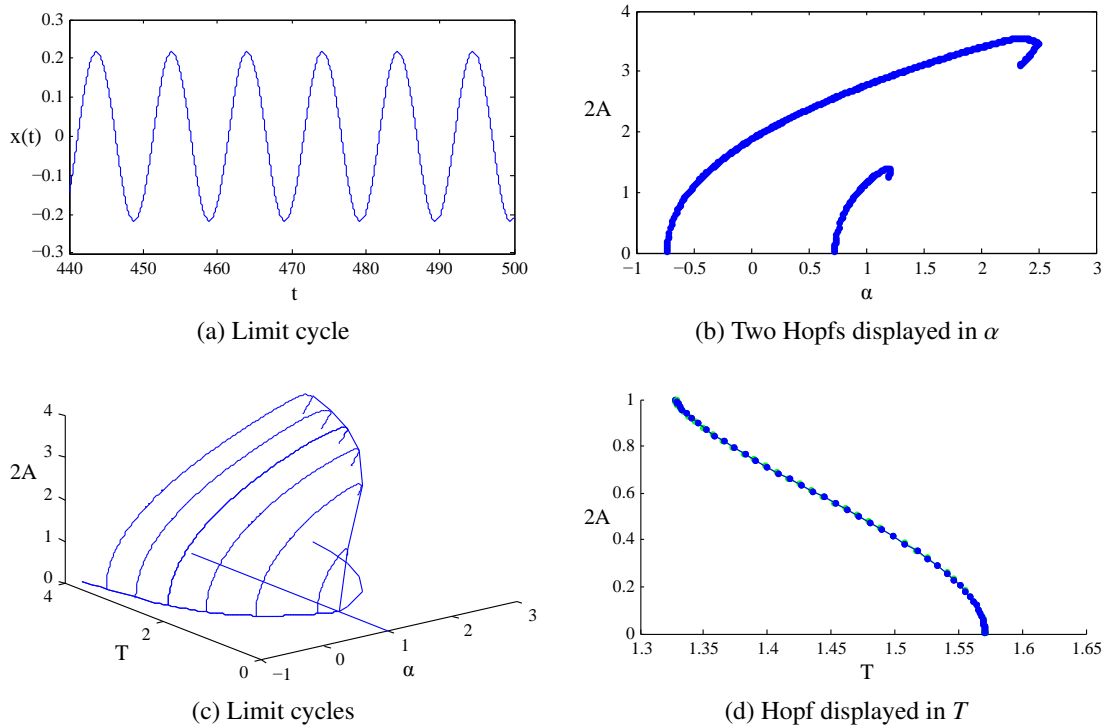- The large delay square wave is not found in simulations for which $\alpha > 3$.

(a) Limit cycle

(b) Two Hopfs displayed in α

(c) Limit cycles

(d) Hopf displayed in T

Fig. 2. (a) Limit cycle obtained by using DDE23 for delay T=4 and α=−0.75. The theoretical values of amplitude and period, namely A=0.2312 and period=0.6614 (see text) agree well with those seen in the simulation; (b) BIFTOOL plots of limit cycle amplitude (x 2) versus α. The smaller curve is for $T = 1.1$ and the larger one is for $T = 3.5$. Note that the limit cycles are born in a Hopf bifurcation and die in a limit cycle fold (as shown numerically), i.e. by merging with an unstable limit cycle in a saddle-node bifurcation of cycles; (c) A surface of limit cycles. Each limit cycle is born in a Hopf and dies in a limit cycle fold. The locus of limit cycle fold points is shown as a space curve, and is also shown projected down onto the α-T plane; (d) BIFTOOL plot showing Hopf off of the equilibrium at $x = \sqrt{\alpha - 1} = 0.7071$ for $\alpha = 1.5$, for varying delay T. Note that Eq. (15) gives the critical value $T_H = \pi/2$.

In this section we offer analytic explanations for these observations.

Since Eq. (4) is invariant under the transformation $x \mapsto -x$, we may refer to the value at the upper edge of the square wave as $x = A > 0$, in which case the value at the lower edge is $x = -A$. Then at a point $x(t)$ on the lower edge, $x(t - T)$ refers to a point on the upper edge, $x(t - T) = A$, and Eq. (4) becomes:

$$0 = -A - (-A)^3 + \alpha(-A) \tag{19}$$

which gives the nontrivial solution

$$A = \sqrt{\alpha + 1} \tag{20}$$

Note that if $\alpha < -1$, this solution cannot exist, no matter what the delay T is.

During a jump down, $x(t - T)$ again takes on the value $\sqrt{\alpha + 1}$, so that Eq. (4) becomes

$$\frac{dx}{dt} = -\sqrt{\alpha + 1} - x^3 + \alpha x \tag{21}$$

Eq. (21) has equilibria at

$$x = -\sqrt{\alpha + 1}, \ x = \frac{\sqrt{\alpha + 1} \pm \sqrt{\alpha - 3}}{2} \tag{22}$$

(a) Square Wave

(b) Amplitudes of T=1.19

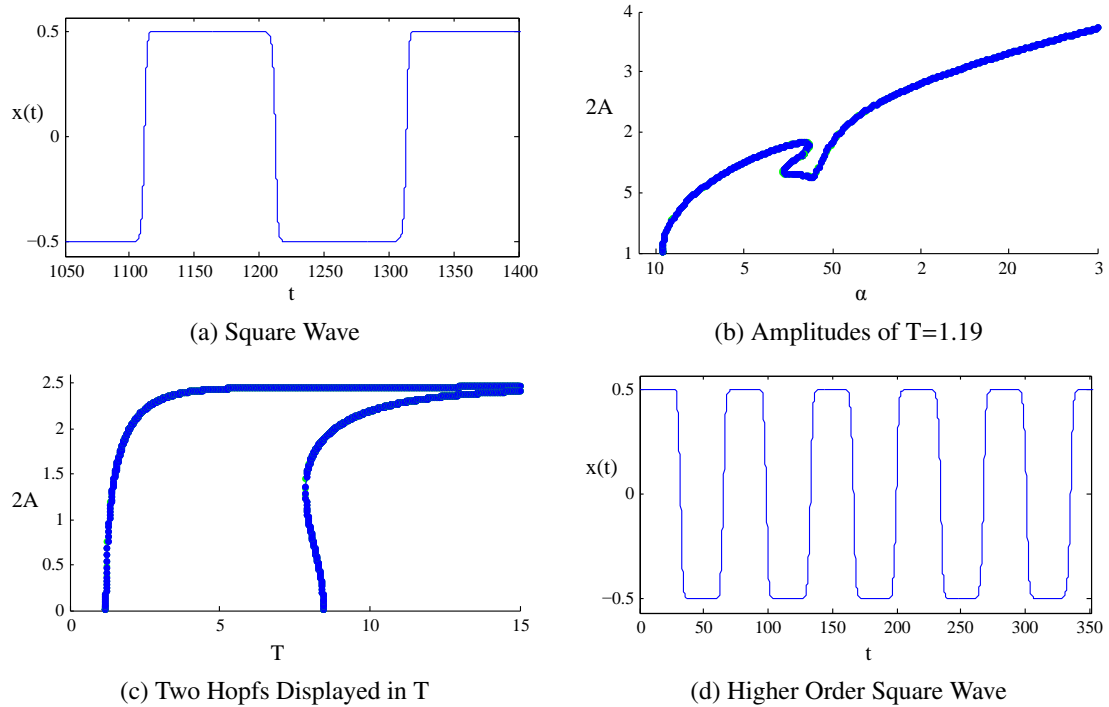(c) Two Hopfs Displayed in T

(d) Higher Order Square Wave

Fig. 3. (a) Limit cycle obtained by using DDE23 for delay $T=100$ and $\alpha=-0.75$. Note the approximate form of a square wave, in contrast to the nearly sinusoidal wave shape for smaller values of delay, cf. Fig. 2(a); (b) Numerical simulation of Eq. (4) using DDE-BIFTOOL. Note that the left portion of the continuation curve is similar to those shown in Figs. 2(b) and 2(c). However the additional bifurcations shown have not been identified. The periodic motions represented by the rest of the branch could not be found using DDE23 and are evidently unstable; (c) DDE-BIFTOOL plots of the limit cycles created by the first two Hopf bifurcations at $x = 0$, found for $\alpha = 0.5$ and increasing T; (d) A higher order square wave for $T = 100$, $\alpha = -0.75$ and $n = 2$. Compare with the base square wave ($n = 1$) in Fig. 3(a)

For $\alpha < 3$ there is only one real root, $x = -A = -\sqrt{\alpha + 1}$.

During the jump down, the variable x starts at $\sqrt{\alpha + 1}$, which acts like an initial condition for the jump according to Eq. (21). The motion continues in x towards the equilibrium at $x = -\sqrt{\alpha + 1}$, which is approached for large time t. Note that the other two equilibria in Eq. (22) lie between $x = -\sqrt{\alpha + 1}$ and $x = \sqrt{\alpha + 1}$ in the case that $\alpha > 3$. Their presence prevents x from approaching $x = -\sqrt{\alpha + 1}$ and thus disrupts the jump, which explains why no square wave limit cycles are observed for $\alpha > 3$.

The foregoing argument assumes that the equilibrium at $x = -\sqrt{\alpha + 1}$ is stable. To investigate the stability of the equilibrium at $x = -\sqrt{\alpha + 1}$, we set

$$x = -\sqrt{\alpha + 1} + y \tag{23}$$

Substituting Eq. (23) into Eq. (21), we obtain

$$\frac{dy}{dt} = -y^3 + 3\sqrt{\alpha + 1}y^2 - (2\alpha + 3)y \tag{24}$$

Linearizing Eq. (24) for small y shows that $x = -\sqrt{\alpha + 1}$ is stable for $\alpha > -3/2$. Since the square wave solution ceases to exist when $\alpha < -1$, the restriction of $\alpha > -3/2$ is not relevant.

5. Discussion

In the foregoing sections we have shown that the delay limit cycle oscillator with self-feedback, Eq. (4), supports a variety of dynamical phenomena, including Hopf and pitchfork bifurcations, limit cycle folds and relaxation oscillations. Numerical explorations using DDE-BIFTOOL have revealed that Eq. (4) exhibits additional bifurcations, Fig. 3(b).

We also note that due to the multivalued nature of arccosine, there are an infinite number of Hopf bifurcation curves in parameter space. Referring to Eqs. (11) and (15), these Hopf bifurcation curves can be generalized to:

$$T_H = \frac{(2\pi n + \arccos \alpha)}{\sqrt{1 - \alpha^2}} \tag{25}$$

$$T_H = \frac{(2\pi n + \arccos(3 - 2\alpha))}{\sqrt{1 - (3 - 2\alpha)^2}} \tag{26}$$

for integer n, where the $n = 0$ case represents the bifurcations already discussed. We use the principal value of arccos in this definition to be consistent with the original equations. These additional bifurcations do not change the overall stability of the equilibria. The related periodic motions appear to be unstable and have not been observed in the results of DDE23 simulation. We can use numerical continuation in DDE-BIFTOOL to trace them for varying delay T ; for instance, Fig. 3(c) shows results for the motions created by the $n = 0$ and $n = 1$ Hopf bifurcations.

For large delay T , we found square waves of higher frequency also existed. The periods of these higher order square waves are given by $\frac{2T}{2n-1}$, where n is an integer and $n = 1$ corresponds to the base square wave previously analyzed. See for example Fig. 3(d) which shows a higher order square wave for which $T = 100$, $\alpha = -0.75$ and $n = 2$. Note that the amplitude of this square wave is the same as that of the base square wave, namely $A = \sqrt{\alpha + 1} = \sqrt{-0.75 + 1} = 1/2$. Note also that both the $n = 2$ higher order square wave of Fig. 3(d) and the base square wave of Fig. 3(a) coexist, each of them corresponding to different initial conditions. In fact, higher order square waves corresponding to larger values of n also coexist. An open question is what is the maximum value of n for which higher order square waves exist? The problem is that as n increases, the period $\frac{2T}{2n-1}$ get smaller, and the assumption that the period is large compared to the jump time is no longer valid.

Each edge of the square wave has length equal to half the period, $\frac{T}{2n-1}$. An analysis similar to that presented above in the section on large delay, for the base case, can be repeated here.

6. Conclusion

In this work we have shown that the diverse nature of the observed dynamics of the delay limit cycle oscillator with self-feedback, Eq. (4), depends on the values of the parameters T and α. This may be illustrated by reference to various regions of the α - T parameter plane. See Fig. 4, where the five regions I, II, II, IV, V are bounded by curves a, b, c, d. Also Fig. 5 shows amplitudes of steady-state motions as a function of α for a constant $T > 1$.

- Curve a is given by the Hopf condition Eq. (11), so that a stable limit cycle is born as we cross from region I to region II.
- Curve b is $\alpha = 1$, and as we pass from region II to region III, a new pair of equilibrium points are born in a pitchfork bifurcation, see Fig. 1(a).
- Curve c is given by the Hopf condition Eq. (15), so that an unstable limit cycle is born in a subcritical Hopf as we cross from region III to IV.
- Curve d is a limit cycle fold, see Fig. 2(c). As we cross from region IV to region V, a stable limit cycle disappears in a fold. Thus region V contains only the three equilibrium points, namely the origin (unstable) and the the arms of the pitchfork (stable).
- Finally, the pitchfork equilibria disappear as we cross from region V to region I.

In summary, we may list the stable dynamical structures which appear in the five regions as follows:

- Region I contains a stable equilibrium at the origin.
- Regions II and III contain a stable limit cycle (which was born in a Hopf off the origin).
- Region IV contains both a stable limit cycle and a pair of stable equilibria (the arms of the pitchfork).
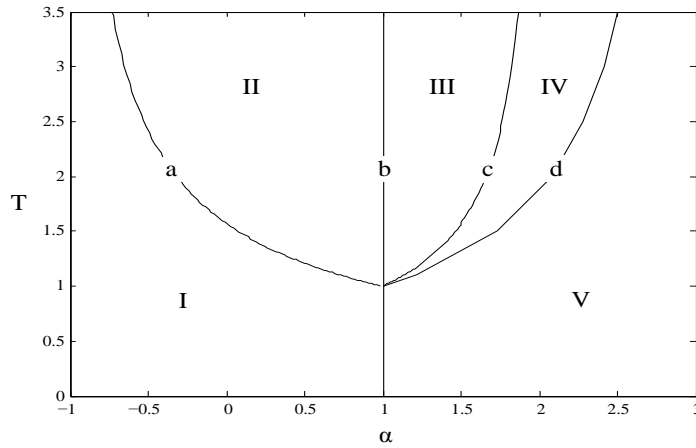- Region V contains a pair of stable equilibria (the arms of the pitchfork).

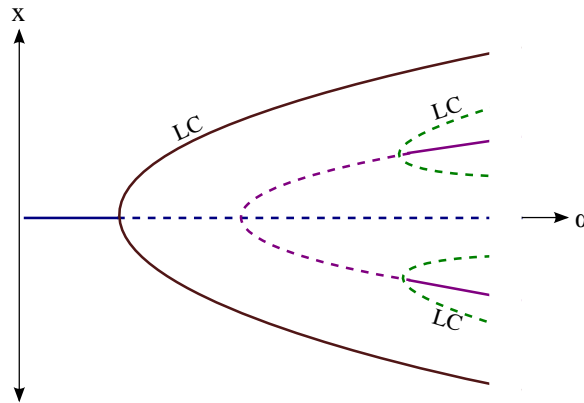Fig. 4. Regions of α - T parameter space and the bifurcation curves which bound them.

Fig. 5. Schematic of equilibrium points and limit cycles seen for $T > 1$ with varying α. The behaviors change as the system crosses the supercritical Hopf (Eq. (11)), pitchfork bifurcation ($\alpha = 1$), and subcritical Hopf (Eq. (15)). Limit cycle fold not shown.

It is to be noted that the foregoing summary has omitted unstable motions (see Fig. 3(b)) as well as motions occurring for large delay (see Figs. 3(a),(d)).

As discussed in the introduction, the delay limit cycle oscillator with self-feedback, Eq. (4), investigated in this paper, is a special solution (the in-phase mode) of the system Eqs. (2),(3). Another special solution is the out-of-phase mode, $x(t) = -y(t)$, governed by the equation:

$$\dot{x} = -x(t - T) - x^3 - \alpha x \tag{27}$$

Eq. (27) is seen to be identical to Eq. (4) but with α replaced by $-\alpha$. Both the in-phase and out-of-phase motions lie in invariant manifolds. If the system is given a general initial condition, numerical simulation has shown that

the resulting motion will approach one or the other of these invariant manifolds. A question which we are currently investigating concerns the stability of these manifolds as a function of the parameters T and α.

Eq. (1), the basic delay limit cycle oscillator upon which this work is based [13,14], is perhaps the simplest example of a system which oscillates due to delay and nonlinearity. We look forward to further investigations based on this system.

References

1. Rand, R.H., and Holmes, P.J.: Bifurcation of Periodic Motions in Two Weakly Coupled van der Pol Oscillators. *Int. J. Nonlinear Mechanics*, **15**, 387–399 (1980).
2. Storti, D.W., and Rand, R.H.: Dynamics of Two Strongly Coupled van der Pol Oscillators. *Int. J. Nonlinear Mechanics*, **17**, 143–152 (1982).
3. Storti, D.W., and Rand, R.H.: Dynamics of Two Strongly Coupled Relaxation Oscillators. *SIAM J. Applied Math.*, **46**, 56–67 (1986).
4. Belair, J., and Holmes, P.: On linearly coupled relaxation oscillators. *Quart. Appl. Math.*, **42**, 193–219 (1983).
5. Chakraborty, T., and Rand, R.H.: The Transition from Phase Locking to Drift in a System of Two Weakly Coupled Van der Pol Oscillators. *International J. Nonlinear Mechanics*, **23**, 369–376 (1988).
6. Wirkus, S., and Rand, R.: Dynamics of Two Coupled van der Pol Oscillators with Delay Coupling. *Nonlinear Dynamics*, **30**, 205–221 (2002).
7. Kuramoto, Y. *Chemical Oscillations, Waves, and Turbulence*. Dover (2003).
8. Cohen, A.H., Holmes, P.J., and Rand, R.H.: The Nature of the Coupling Between Segmental Oscillators of the Lamprey Spinal Generator for Locomotion: A Mathematical Model. *J. Math. Biology*, **13**, 345–369 (1982).
9. Rand, R.H., Cohen, A.H., and Holmes, P.J.: Systems of Coupled Oscillators as Models of Central Pattern Generators. In: Cohen, A.H. (ed.) Chapter 9 in *Neural Control of Rhythmic Movements in Vertebrates*, pp. 333–368. John Wiley and Sons (1988).
10. Strogatz, S.H., and Mirollo, R.E.: Stability of Incoherence in a Population of Coupled Oscillators. *Journal of Statistical Physics*, **63**, 613–635 (1991).
11. Lazarus, L. and Rand, R.: Dynamics of a System of Two Coupled Oscillators which are Driven by a Third Oscillator. *Journal of Applied Nonlinear Dynamics*, **3**(3), 271–282 (2014).
12. Yeung, M.K.S., and Strogatz, S.H.: Time Delay in the Kuramoto Model of Coupled Oscillators. *Phys. Rev. Let.*, **82**, 648–651 (1999).
13. Rand, R.H.: *Lecture Notes in Nonlinear Vibrations*, published online by the Internet–First University Press: http://ecommons.library.cornell.edu/handle/1813/28989 (2012)
14. Rand, R.: Differential–delay equations. In: Luo, A.C.J., Sun, J.-Q. (eds.) Chapter 3 in *Complex Systems: Fractionality, Time–delay and Synchronization*, pp. 83–117. Springer, Berlin (2011).
15. Verdugo, A., Rand, R.: Hopf bifurcation formula for first order differential–delay equations. *Commun. Nonlinear Sci. Numer. Simul.*, **12**, 859–864 (2007).
16. Engelborghs, K., Luzyanina, T., Roose, D.: Numerical bifurcation analysis of delay differential equations using DDE–BIFTOOL. *ACM Trans. Math. Softw.*, **28**(1) 1–21 (2002).
17. Engelborghs, K., Luzyanina, T., Samaey, G.: DDE–BIFTOOL v. 2.00: a Matlab package for bifurcation analysis of delay differential equations. Technical Report TW–330, Dept. Comp. Sci., K.U.Leuven, Leuven, Belgium (2001).
18. Lazarus, L., Davidow, M., Rand, R.: Dynamics of a delay limit cycle oscillator with self–feedback. *Nonlinear Dynamics*, **82** (1): 481–488 (2015).